Journal of Theoretical and Applied Information Technology

31st August 2023. Vol.101. No 16

ISSN: 1992-8645 www.jatit.org E-ISSN: 1817-3195

A NOVEL OPTIMIZATION-BASED APPROACH FOR HARMONIC ASSESSMENT IN HYBRID MICROGRIDS

DEVIKA RANI MOTUKURI [1]* P.S.PRAKASH [2] M.VENU GOPALA RAO [3]

[1] Research Scholar, Department of Electrical Engineering, Faculty of Engineering & Technology, Annamalai University, Annamalai Nagar ,Chidambaram, Tamil Nadu-608002, India
[2]Assistant Professor, Department of Electrical Engineering, Annamalai University, Annamalai Nagar, Chidambaram, Tamil Nadu-608002, India.
[3]Professor, Department of Electrical & Electronics Engineering, QIS College of Engineering & Technology, Ongole, Andhra Pradesh, India

* Corresponding author's Email: devikamothukuri@gmail.com

ABSTRACT

Hybrid microgrids have shown great promise in recent years as a way to deal with the difficulties of combining renewable energy sources with conventional power plants in contemporary power grids. However, the performance and stability of such microgrids might be negatively impacted by the existence of harmonic disturbances. Effective control solutions are required to reduce harmonic distortions and guarantee reliable power transmission. This research suggests a Proportional-Integral-Derivative (PID) controller based on Gray Wolf Optimization (GWO) be used to evaluate harmonics in hybrid microgrids. Inspired by the pack dynamics of grey wolves, the GWO algorithm is a robust and simple optimization method with quick convergence rates. This research aim is to optimize the PID controller settings in real-time to reduce harmonic distortions in the microgrid system by combining the GWO method with the PID controller. A thorough simulation model of a hybrid microgrid, including multiple distributed energy supplies, energy storage devices, and loads, is used to assess the effectiveness of the suggested control technique. We compare the GWO-based PID controller to traditional PID controllers and various optimization approaches like particle swarm optimization to demonstrate its harmonic reduction ability. Due to enhanced harmonic evaluation, the GWO-based PID controller increases the power quality and decreases the harmonic distortion, according to simulations. This controller is ideal for hybrid microgrids since it adapts to changing system conditions and load needs. This work shows that the GWO-based PID controller can efficiently mitigate harmonics and improve renewable-integrated power system performance, contributing to hybrid microgrid control strategies.

Keywords: *Renewable Energy Sources, Power Quality, Gray Wolf Optimization, Particle Swarm Optimization, PID Controller, Total Harmonic Distortion.*

1. INTRODUCTION

1.1. Background and Motivation

The utilization of hybrid microgrids and the incorporation of renewable energy sources have become increasingly common place in the power systems industry in recent years [1-4]. Hybrid microgrids are able to provide a more stable and long-lasting power supply since they utilize both renewable and conventional energy sources.

Microgrids are distributed power networks that can provide power on their own or in tandem with the larger utility grid [7]. They provide hope for lowering energy bills, strengthening the reliability of the power grid, and cutting carbon emissions. However, microgrids confront a significant obstacle in the form of harmonics in the power stream, which can increase THD and cause other power quality problems [6]. As a result, hybrid microgrids are being considered as a viable option for lowering THD and enhancing power quality. The purpose of this paper is to introduce hybrid microgrids and discuss their potential usefulness in

lowering THD. THD can be lowered by the usage of hybrid microgrids that incorporate renewable energy sources like solar and wind. When compared to traditional generators, the power produced by these alternatives is cleaner and has fewer harmonic. Batteries and capacitors, two types of energy storage systems, can also be used to dampen power spikes and drop the total harmonic distortion (THD).

To lower total harmonic distortion (THD) and boost power quality in microgrids, hybrid microgrids are a possible alternative. However, power quality issues, such as harmonic distortion and poor power factor, can arise in hybrid microgrids due to the integration of these various energy sources and the existence of nonlinear loads [5].

Optimization-based techniques have emerged as viable approaches to resolving issues with power quality. Gray Wolf Optimization (GWO) [8-10] is one such method that has attracted attention for its capacity to handle difficult optimization problems in a manner reminiscent of the social structure and hunting strategies of gray wolves. The optimization and control of power systems are two areas where GWO has proven to be useful [11].

Using GWO is a novel way to optimize system performance and reduce harmonic distortions in the context of harmonic evaluation in dispatched power mode hybrid microgrids. Using GWO, the hybrid microgrid system's control settings and dispatch algorithms can be adjusted to reduce harmonics and boost power quality. This optimization-based method makes it possible for hybrid microgrids operating in dispatched power mode to effectively and efficiently deal with power quality challenges [12-15].

1.2 Objectives of the Study

To analyze harmonics and evaluate power quality in hybrid microgrids, we provide a new optimization-based method. To fine-tune the HSHAPF's Proportional Integral Derivative (PID) controller's settings, we apply the GWO method. In the face of nonlinear and unbalanced loads, the goal is to reduce harmonic distortions and boost power quality overall.

1.3 Scope and Significance

The scope of this topic includes the development and application of an innovative optimization technique to evaluate and mitigate harmonics within a hybrid microgrid system. The approach focuses on leveraging optimization methods to enhance the power quality and harmonic performance of the microgrid under various operating conditions. The approach involves the identification, analysis, and quantification of harmonic distortions present in the hybrid microgrid.

This paper's remaining sections are structured as follows. In Section 2, we will look into the research done on hybrid microgrids on optimization-based harmonic assessment methods. Methodology and mathematical formulation of the GWO-based harmonic analysis method proposed in Section 3 are presented. The evaluation and results of the simulation are discussed in Section 4. The report finishes with a brief summary and some recommendations for future study in Section 5.

2. LITERATURE STUDY

2.1 Hybrid Microgrids and Harmonic Distortions with optimization

Harmonic distortions in microgrids can lead to various power quality issues such as voltage and current distortions, increased total harmonic distortion (THD), and reduced power factor [16-19]. These issues can affect the performance and efficiency of electrical devices and cause operational problems. By employing optimization-based harmonic assessment, it becomes possible to identify and mitigate the sources of harmonics, thereby improving power quality and ensuring the reliable operation of microgrid systems. By assessing harmonics and identifying their sources, optimization algorithms can determine the optimal placement of power electronic devices, such as filters or compensators, to mitigate harmonics [20]. This helps in achieving effective resource allocation and utilization, reducing costs, and enhancing overall system performance.

In the study conducted by Jia et al. (2018) [21], an optimal harmonic suppression strategy for a hybrid microgrid based on an adaptive genetic algorithm was proposed. Through the utilization of an adaptive genetic algorithm, the proposed optimal harmonic suppression strategy demonstrated significant improvements in harmonic suppression and power quality enhancement in a hybrid microgrid. The genetic algorithm was able to adaptively optimize the harmonic suppression parameters based on the system's operating conditions and load characteristics. An optimal

harmonic control strategy for a hybrid AC/DC microgrid based on particle swarm optimization (PSO) was proposed in [22].

The application of the improved particle swarm optimization (PSO) algorithm in the harmonic assessment and optimization of the hybrid microgrid proved to be successful in mitigating harmonics and enhancing the power quality. The proposed algorithm [18] incorporated modifications to the conventional PSO, such as the introduction of local search and adaptive inertia weight, to enhance its convergence and search capabilities. In [13] authors investigated the optimal operation of a hybrid AC/DC microgrid using the Gray Wolf Optimization (GWO) algorithm. The application of the Gray Wolf Optimization (GWO) algorithm for the optimal operation of a hybrid AC/DC microgrid proved to be effective in achieving improved system performance. The GWO algorithm was utilized to optimize the power sharing and control strategies of the microgrid components, including the renewable energy sources, energy storage systems, and converters. The harmonic assessment and optimization of a hybrid microgrid considering uncertainties are the important criteria in [17].

Figure 1: Schematic diagram of RES-based HSHAPF

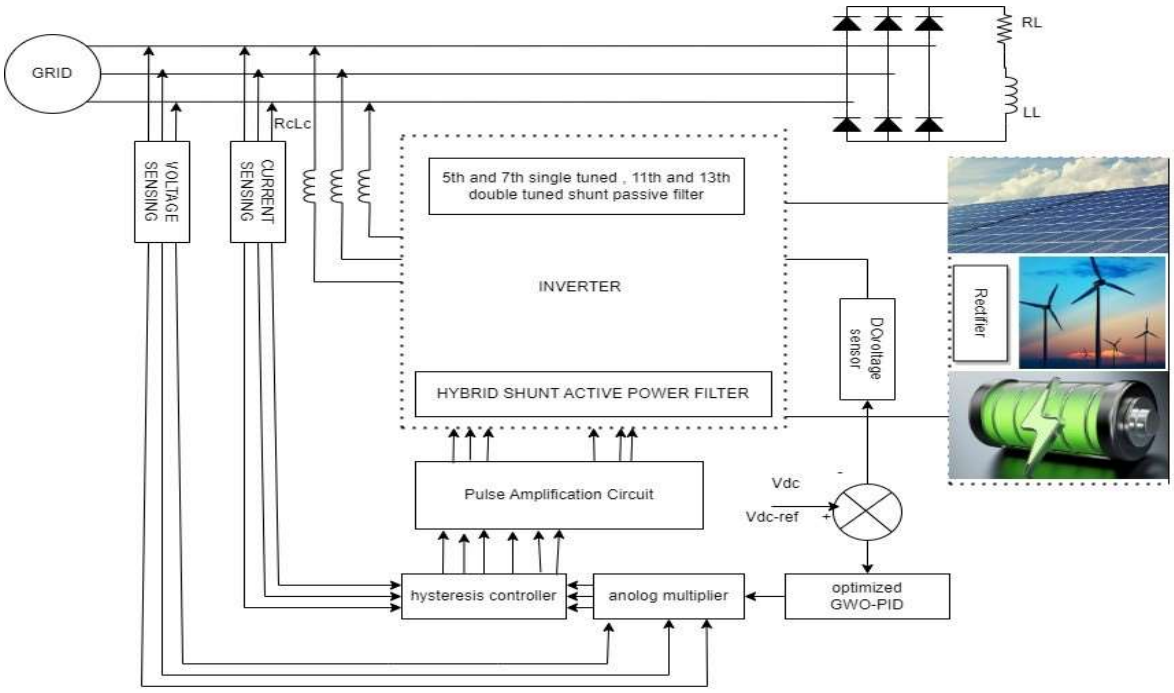

The research proposed a comprehensive approach for the harmonic assessment and optimization of a hybrid microgrid that considers uncertainties. The approach utilized a combination of probabilistic modeling techniques, such as Monte Carlo simulation, and optimization algorithms to assess and optimize the harmonic performance of microgrid under uncertain operating conditions. In [4] Zhang et al. (2020), the authors focused on the optimization strategy for an active harmonic filter (AHF) in an AC/DC hybrid microgrid based on an improved ant colony algorithm. The research proposed an optimization strategy for the AHF in the AC/DC hybrid microgrid based on an improved ant colony algorithm. The algorithm was designed to optimize the control parameters of the AHF and achieve efficient harmonic suppression while considering the operating conditions and load characteristics of the microgrid.

In [23] authors proposed the utilization of the Artificial Bee Colony (ABC) algorithm for optimizing the placement of shunt active power filters (SAPFs) in microgrids. Here authors compared the performance of the ABC algorithm with other optimization techniques, such as the Genetic Algorithm (GA) and Particle Swarm Optimization (PSO). The results indicated that the ABC algorithm outperformed these techniques in terms of convergence speed and solution quality. Wang et al in [24], the Differential Evolution (DE)

algorithm to determine optimal locations and sizes of capacitors.

2.2 PID Control in Microgrid Systems

Poor tuning is a common problem with traditional proportional-integral-derivative (PID) tuning methods, but this problem is solved by the contemporary optimization methodology based on performance indices, which results in optimal tuning and enhanced performance [27]. By comparing the frequency variations of the microgrid system with and without a PID controller, one can see that the PID controller was successful in stabilizing the system and dampening the frequency changes to some extent. The hybrid PSO-GSA algorithm was employed for the best possible outcomes. It was found that the proposed smart controller outperformed the particle swarm controller in this simulation [28].

A microgrid's efficiency is largely predicated on how stable and reliable it is. Solutions based on fractional regulators show promise for maintaining reliable microgrid operations. For both single and dual area AC microgrids, this article suggests a supplementary Load Frequency Control (LFC) based on Fractional order Proportional-Integral-Derivative (FOPID) [29]. Since loads on a power grid are always shifting, frequency variation is a major cause for concern. The frequency instability is a problem for the stand-alone hybrid microgrid that uses wind/solar systems produced with MPPT algorithms. The suggested standalone hybrid microgrid employs PID controllers to reduce frequency variation. Ziegler-Nichols is used to find the best settings for the PID controller's parameters. [30] When the coefficients of a Proportional-Integral-Derivative (PID) controller are set correctly, the controller is easy to use and produces good results. Particle swarm optimization, genetic algorithm, imperialist competitive algorithm, and selfish herd optimization are the four evolutionary algorithms used in [31] to determine the PID controller coefficients and put to the test in the microgrid's frequency and voltage regulation.

3. METHODOLOGY OF PROPOSED METHOD

3.1 Microgrid Configuration and Components

As shown in Figure 1, which depicts the connection between the RES and HSHAPF to the grid, HSHAPF is implemented in this article by combining the LC passive filter and voltage source PWM converter.Table-1, 2, 3 illustrates the design parameters.

Table: 1 Solar

Module Type: 1soltech1 1sth-230-P

S.NO	PARAMETERS	VALUES
1	MAX POWER	228.735W
2	Cells per module	60
3	OC voltage	29.9V
4	SC current	8.18A
5	Voltage at max power point	29.9V
6	Current at max power point	7.65A
7	Irradiance	1000
8	Frequency	50Hz

Table: 2 Wind Turbine Parameters

S.NO	PARAMETERS	VALUES
1	Base wind speed	12m/s
2	Base rotational speed	0.4m/s
3	Maximum pitch angle	45 deg
4	Maximum rate of change of pitch angle	2 deg/s
5	Universal Bridge	

Table: 3 Battery Parameters

S.NO	PARAMETERS	VALUES
1	Type	Nickel-Metal-Hydride
2	Initial state-of-charge	100%

3	Battery response time	30 Sec
4	Nominal voltage	1.5 V
5	Rated capacity	6.5 Ah

3.2 Load Modeling and Harmonic Generation

Nonlinear and unbalanced loads are used to evaluate the robustness of this architecture. Both filters' features are optimized for peak performance in a wide range of environments. The battery, DC link, and switches with antiparallel diodes are modeled as storage systems in the design to eliminate harmonics. At PCC, a voltage source converter is used to inject compensating current, reducing the impact of harmonics. Both active and passive filters are modelled into the system to reduce harmonics and get around the PWM converter's power rating. In this case, the PWM converters are designed with power MOSFETs, which reduces manufacturing costs. Harmonics can be eliminated at the PCC by injecting harmonic current of equal and opposite magnitude, which also boosts PQ throughout the distribution network.

Table 4: Load data for Microgrid system

Load Name	Load Type	Rating of the load(kVA)	Power factor
Load12	Linear Load	800	0.8
Load 14	Linear Load	1600	0.8
Load3	Non-Linear Load	320	1
Load4	Unbalanced load	30	0.85
Load5	Unbalanced load	40	0.9

In this paper, we introduce a PID controller and a proposed controller that together achieve the best total harmonic distortion (THD) reduction under nonlinear load and unbalanced load compared to no filter, a passive filter (PF), and an active power filter (APF), respectively. The key contribution of this study is as follows: The DG consists of photovoltaic panels, wind turbines, and battery storage. When there is a surplus of energy created, it can be stored in batteries and later used to offset the necessary load. The system is designed to work together as a whole. When the PCC is connected, the dynamic performance is measured under different loads. The system's stability is compromised by the harmonics created by this integration. To effectively address the PQ concerns and lower the THD, a new PID controller is presented, and a metaheuristic algorithm called Gray wolf optimization (GWO) is introduced to generate the best optimal pulse for the controller. Both passive and active filters were used in the creation of the proposed modeling. The filter's compensating properties are enhanced by the developed model, mitigating drawbacks associated with active and passive filters.

4. MATHEMATICAL MODELLING OF THE PROPOSED SYSTEM

A set of n harmonics with n = {1,2,3,....N} is proposed. At the same position, components are found, and they are current I_l(t) and Voltage V_s (t), which can be expressed as the equations (1) to (7) that follows Figures 6, 7 depict the mathematical modelling of the controller.

$$V_s(t) = \begin{bmatrix} V_{S1} \\ V_{S2} \\ V_{S3} \end{bmatrix} = \begin{bmatrix} \sum_{n=1}^{N} V_{sn1} \sin\left(n(\omega t)\right) \\ \sum_{n=1}^{N} V_{sn2} \sin\left(n(\omega t - 120°)\right) \\ \sum_{n=1}^{N} V_{sn3} \sin\left(n(\omega t - 240°)\right) \end{bmatrix} \quad (1)$$

The real power delivered by the grid Ps should be similar to the grid power provided for compensating at a high power factor using the below equation (2)

$$P_S = P_L + P_l - P = \frac{3}{2} V_{S1} \quad (2)$$

($I_{Ln1}, I_{Ln2}, I_{Ln3}$) are load current peak values; (V_{sn1}, V_{sn2}, V_{sn3}) are PCC voltage peak values; and $\emptyset_{n1}$, $\emptyset_{n2}$, and $\emptyset_{n3}$ are harmonic component phase angles of the nth order.

$$i_L(t) = \begin{bmatrix} i_{l1} \\ i_{l2} \\ i_{l3} \end{bmatrix} = \begin{bmatrix} \sum_{n=1}^{N} I_{Ln1} \sin(n\omega t - \emptyset_{n1}) \\ \sum_{n=1}^{N} I_{Ln2} \sin(n(\omega t - 120°) - \emptyset_{n2}) \\ \sum_{n=1}^{N} I_{Ln3} \sin(n(\omega t + 120°) - \emptyset_{n3}) \end{bmatrix} \quad (3)$$

$$I^*_{s1} = \frac{2P_s}{3V_{s1}} \quad (4)$$

$$\begin{aligned} I^*_{sx}(t) &= I^*_{s1} u_{sx} \\ I^*_{sy}(t) &= I^*_{s1} u_{sy} \\ I^*_{sz}(t) &= I^*_{s1} u_{sz} \end{aligned} \quad (5)$$

$$\begin{aligned} u_{sx}(t) &= u_a(t) \\ u_{sy}(t) &= -\frac{1}{2} u_a(t) + \frac{\sqrt{3}}{2} u_b(t) \\ u_{sz}(t) &= -\frac{1}{2} u_a(t) - \frac{\sqrt{3}}{2} u_b(t) \end{aligned} \quad (6)$$

where the real loss of power is P_l , the actual power delivered by the RES is P, and the real power of the load is P_L; as a result, the maximum value of the basic aspect of typical point voltage is a key component, and I_s* is an essential component and is the source current component expressed in the above equation.

Distance between neighbouring reference currents is represented by the equations ua(t) = sin t and ub(t) = cost. The HCC (ica, i_{cb}, icc) receives feedback from the current inverter and the standard inverter current errors and modifies the duty ratio of the PWM inverter according to the following equation.

$$\begin{aligned} \Delta ica &= I*C_1(t) - ic1 \\ \Delta i_{cb} &= I*C_2(t) - ic2 \\ \Delta icc &= I*C_3(t) - ic3 \end{aligned} \quad (7)$$

Determined by the difference between the real and perceived currents of the inverter, the hysteresis regulator regulates and modulates pulse in both gate actuators of a grid-connected adapter. In phase A of the inverter, the S1 switch is on, while Δic1 > Hb and S4 are off, and vice versa if Δic1 < Hb. Hb the hysteresis band's width. The period of the switching pulses for either leg will be the same.

5. CONTROL STRUCTURE OF HYBRID SHUNT ACTIVE POWER FILTER

Harmonic suppression and attenuation performance is highly dependent on the HSAPF's control mechanism. In a hybrid shunt active power filter, the lower order harmonics are filtered out by a passive filter and the higher order harmonics are smoothed out by an active filter. The harmonic current is cancelled out by a compensation current generated by the active filter, which is comprised of a power electronics converter and a control system. A feedback loop in the control system measures the harmonic current and then uses that information to calculate the compensating current.

A power source inverter, a GWO controller, and passive and active filters make up the HSAPF control structure in a hybrid microgrid with GWO. In order to keep the voltage steady and the THD low, the HSAPF's control settings are optimised with the help of the GWO algorithm. As shown in Figures 2 and 3, compensating currents are generated using the p-q theory, which is predicated on the transformation of a-b-c coordinates into α-β-0 coordinates and α-β-0 conversations into a-b-c parameters, also known as Clark's transformation and the inverse transformation, respectively. When performing a harmonic analysis on a three-phase system, Clarke's transformation is also commonly utilized. When building filters or mitigation measures for harmonic distortion, it is essential to first isolate the fundamental frequency components and then the harmonic frequency components.

The following equations describe the transformation from three-phase source voltage and load current to the dq0 stationary reference frame.

$$\begin{bmatrix} V^{s0} \\ V^{s\alpha} \\ V^{s\beta} \end{bmatrix} = \sqrt{\frac{2}{3}} \begin{bmatrix} \frac{1}{\sqrt{2}} & \frac{1}{\sqrt{2}} & \frac{1}{\sqrt{2}} \\ 1 & -\frac{1}{2} & -\frac{1}{2} \\ 0 & \frac{\sqrt{3}}{2} & -\frac{\sqrt{3}}{2} \end{bmatrix} \begin{bmatrix} V^{sa} \\ V^{sb} \\ V^{sc} \end{bmatrix} \quad (8)$$

$$\begin{bmatrix} I^{l0} \\ I^{l\alpha} \\ I^{l\beta} \end{bmatrix} = \sqrt{\frac{2}{3}} \begin{bmatrix} \frac{1}{\sqrt{2}} & \frac{1}{\sqrt{2}} & \frac{1}{\sqrt{2}} \\ 1 & -\frac{1}{2} & -\frac{1}{2} \\ 0 & \frac{\sqrt{3}}{2} & -\frac{\sqrt{3}}{2} \end{bmatrix} \begin{bmatrix} I^{La} \\ I^{Lb} \\ I^{Lc} \end{bmatrix} \quad (9)$$

Using phase-neutral voltages and load currents, the instantaneous values of the considered and unconsidered powers can be calculated.

$$\begin{bmatrix} P \\ Q \end{bmatrix} = \begin{bmatrix} V^{s\alpha} & V^{s\beta} \\ -V^{s\beta} & V^{s\alpha} \end{bmatrix} \begin{bmatrix} I^{l\alpha} \\ I^{l\beta} \end{bmatrix} \quad (10)$$

$$\begin{bmatrix} I^{Ra} \\ I^{Rb} \\ I^{Rc} \end{bmatrix} = \sqrt{\frac{2}{3}} \begin{bmatrix} 1 & 0 \\ -\frac{1}{2} & \frac{\sqrt{3}}{2} \\ -\frac{1}{2} & -\frac{\sqrt{3}}{2} \end{bmatrix} \begin{bmatrix} I^{R\alpha} \\ I^{R\beta} \end{bmatrix} \quad (11)$$

In the shunt active filter, the actual and reactive power is determined using the above equations. A proportional, integral, and derivative (PID) controller is a type of feedback control system that uses these three regulatory actions to bring the system's output to some predetermined value, known as a setpoint.

A mathematical expression for the PID controller's control algorithm is as follows:

$$u(t) = K_p{}^* e(t) + K_i{}^* \int e(t) + K_d{}^* de(t)/dt \quad (12)$$

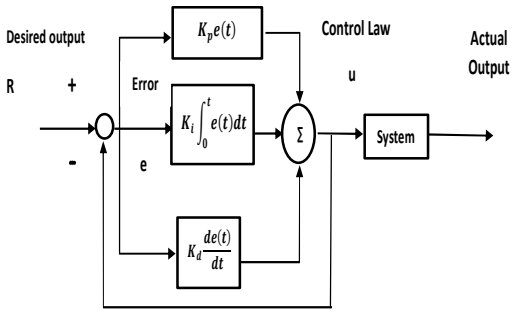

Figure 2: proportional integral derivative

Kd is the derivative gain
Where: u(t) is the controller output at time t
Kp is the proportional gain
The error, denoted by e(t), is defined as the departure from the target value of the control variable at time t. variable The error growth rate, de(t)/dt. The integral gain Ki controls the rate at which the output varies in reaction to the accumulated error over time, while the proportional gain Kp controls the size of the output response to variations in the error. How quickly the output adapts to errors that occur over time is set by the derivative gain Kd.

$$G_{p1}(s) = k_{p1} + \frac{k_{i1}}{s} = k_{p1} \left(1 + \frac{1}{T_{I1}s}\right) \quad (13)$$

$$G_{q2}(s) = k_{q2} + k_{d1}s = \mathrm{k_{q1}}(1 + T_{J2}s) \quad (14)$$

$$G_{r3}(s) = k_{r3} + \frac{k_{i2}}{s} = k_{r2}(1 + \frac{1}{T_{K2}s}) \quad (15)$$

$$G_{s4}(s) = k_{s4} + k_{d2}s = k_{s2}(1 + T_{L2}s) \quad (16)$$

$$G_{p1}(s) = \frac{k_1}{\tau_1 s - 1} e^{-\theta_1 s} \quad (17)$$

$$G_{p2}(s) = \frac{k_2}{\tau_2 s + 1} e^{-\theta_2 s} \quad (18)$$

$$\vec{D} = | \overrightarrow{CX_p}(t) - \vec{X}(t) | \quad (19)$$

$$\vec{X}(t+1) = \overrightarrow{X_p}(t) - \vec{A}\vec{D} \quad (20)$$

6. GRAY WOLF OPTIMIZATION TECHNIQUE

The meta-heuristic optimisation algorithm Grey Wolf Optimizer (GWO) was inspired by the hunting techniques of grey wolves. With the goal of increasing system efficiency, it has been successfully applied to a wide variety of technical problems.

6.1 Encircling the Prey: The grey wolves enclosing the prey while hunting. The encircling of grey wolves can be modelled using

$$\vec{A} = 2\vec{a}\overrightarrow{r_x} - \vec{a} \quad (21)$$

$$\overrightarrow{C_a} = 2\overrightarrow{r_x} \quad (22)$$

Where t indicates the iteration, $\overrightarrow{A}$ and $\overrightarrow{C}$ represents the constant (coefficient) vectors, position vector of prey and wolf are represented by $\overrightarrow{X_P}$ and $\overrightarrow{X}$ respectively.

The value of $\overrightarrow{a}$ declines proportionally from two to zero over the entire iterations. $\overrightarrow{r_1}$ and $\overrightarrow{r_2}$ are the arbitrary random vectors taken between 0 and 1.

6.2 Hunting Mechanism of Grey Wolves: The alphas, betas, and deltas typically lead the hunt because they are better able to anticipate where the prey will be. The remaining mediators in the exploration process must adjust to the position of the best one.

Various design equations related to the objective function are given from (23) to (33)

$$\overrightarrow{D_{a\propto}} = |\overrightarrow{C_1}\overrightarrow{X_{v\propto}} - \vec{X}| \quad (23)$$

$$\overrightarrow{D_{a\beta}} = |\overrightarrow{C_2}\overrightarrow{X_{v\beta}} - \vec{X}| \quad (24)$$

$$\overrightarrow{D_{a\delta}} = |\overrightarrow{C_3}\overrightarrow{X_{v\delta}} - \vec{X}| \quad (25)$$

$$\vec{X}(t+1) = \left(\frac{\overrightarrow{X_1}+\overrightarrow{X_2}+\overrightarrow{X_3}}{3}\right) \quad (26)$$

$$\sqrt{\sum_{i=1}^{n}(x_i - y_i)^2} \quad (27)$$

$$J_{min} = \sqrt{(x_{i1} - y_{a1})^2 + (x_{j2} - y_{a2})^2 + (x_{k3} - y_{a3})^2} \quad (28)$$

$$IAE = \int_0^{\infty} |e(t)|dt \quad (29)$$

$$Y = \sum_{I=1}^{\infty} |u_{i+1} - u_i| \quad (30)$$

$$\overrightarrow{X_\alpha} = \overrightarrow{X_{v\alpha}} - \overrightarrow{A_1 D_{v\alpha}} \quad (31)$$

$$\overrightarrow{X_\beta} = \overrightarrow{X_{v\beta}} - \overrightarrow{A_2 D_{v\beta}} \quad (32)$$

$$\overrightarrow{X_\gamma} = \overrightarrow{X_{v\delta}}\overrightarrow{A_3}\overrightarrow{D_{v\delta}} \quad (33)$$

ISSN: 1992-8645

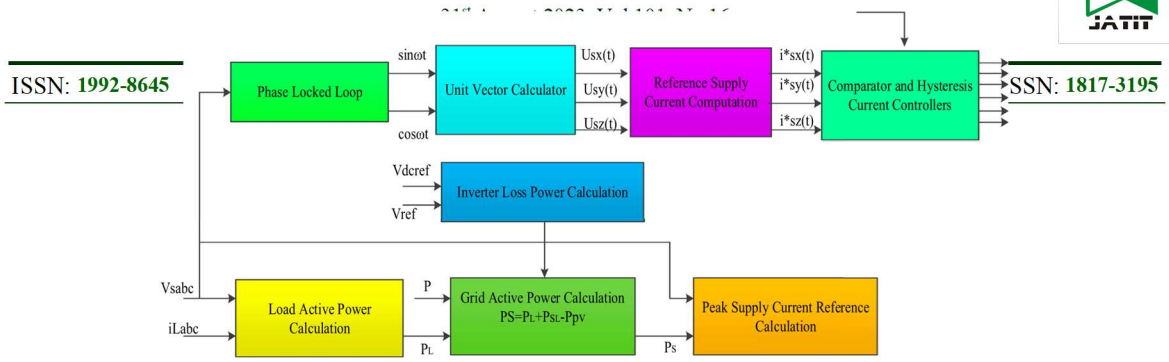

FIGURE 6 | Control structure of the proposed system.

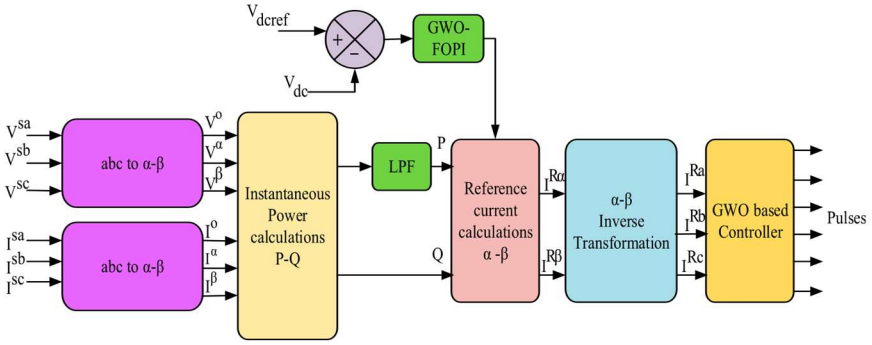

FIGURE 7 | HSHAPF control structure.

The procedure of the suggested approach is as follows:

Step 1: Create the populations.

Step 2: Using Eqs 15, 16, calculate the values of Y, a, and Z.

Step 3: A random location is created from the Search agent.

Step 4: The fitness values of gray wolves are computed using an objective function.

Step 5: The position of the gray wolves as well as the parameters A, a, and C, are changed.

Step 6: Using fitness calculations, the optimal option for the next generation is selected.

Step 7: xα, xβ, and xγ are all updated.

Step 8: If the halting condition is not met, the preceding steps are repeated.

Step 9: The controller's optimal settings are determined for the selected objective of harmonic reduction.

The algorithmic processes of searching, updating, and exploiting are depicted in the flowchart below.

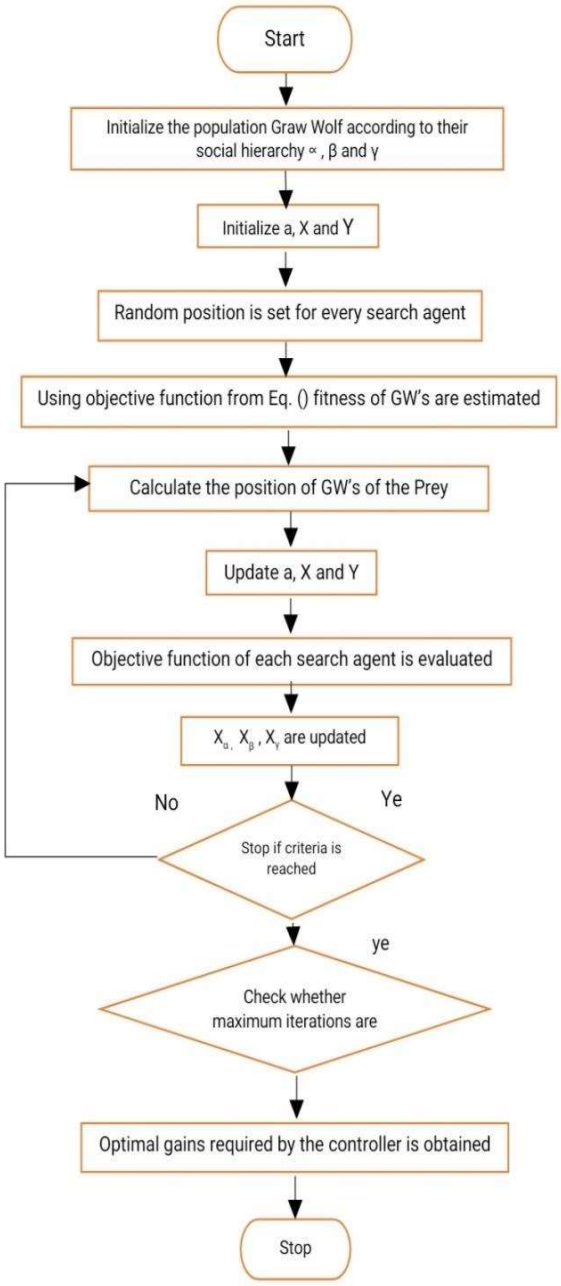

Figure 5: Flow chart of GWO

7. PERFORMANCE EVALUATION HARMONIC ASSESSMENT METRICS

Overall, Performance Evaluation Metrics provide a structured and systematic approach to assessing power quality, enabling better understanding, decision making, and improvement of power systems. Table 5 summarizes how harmonics in a Hybrid microgrid can be evaluated with the help of several indicators.

Table 5 Summary of Various metrics

Metric	Calculation/Assessment
Total Harmonic Distortion (THD) Reduction	THD Reduction (%) = ((Initial THD - Optimized THD) / Initial THD) * 100
Voltage Harmonic Amplitude Reduction(%VTHD)	Amplitude Reduction (%)=((Initial Amplitude - Optimized Amplitude) / Initial Amplitude) * 100
Current Harmonic Amplitude Reduction(%ITHD)	Amplitude Reduction (%) = ((Initial Amplitude - Optimized Amplitude) / Initial Amplitude) * 100
Voltage THD Reduction	THD Reduction (%) = ((Initial THD - Optimized THD) / Initial THD) * 100
Current THD Reduction	THD Reduction (%) = ((Initial THD - Optimized THD) / Initial THD) * 100

The following phases outline the process from problem conception through maximum THD reduction within THD restrictions.

1. Objective Function:

$$J = J_H + J_V + J_C \quad (34)$$

The objective function J represents the sums of individual harmonic distortion terms for the harmonic assessment.

2. Harmonic Distortion Error Term:

$$J_H = K_H \times (THD - THD\_ref)^2 \quad (35)$$

The harmonic distortion error term J_H is calculated based on the difference between the total harmonic distortion (THD) and a reference THD (THD_ref), multiplied by the harmonic distortion gainK_H.

3. Voltage Harmonic Error Term:

$$J_v = K_v^*(v_h - v_{href})^2 \quad (36)$$

The voltage harmonic error term Jv is computed based on the difference between the harmonic voltage (v_h) and a reference harmonic voltage (v_{href}), multiplied by the voltage harmonic gainK_v.

4. Current Harmonic Error Term:

$$J_c = K_c^*(i_h - i_{href})^2 \quad (37)$$

The current harmonic error term Jc is determined by the difference between the harmonic current (i_h) and a reference harmonic current (i_{href}), multiplied by the current harmonic gain Kc.

5. GWO Optimization Process:

Initialize the positions of the alpha, beta, and delta wolves as potential solutions to the optimization problem.

Evaluate the fitness (objective) function J for each wolf using the current PID gains.

Update the positions of the wolves based on their fitness values and the GWO algorithm. Repeat the evaluation and update step for specified number of iterations or until convergence is achieved

Select the best solution (wolf) that provides the optimal PID gains for harmonic assessment in the hybrid microgrid.

6. Harmonic Distortion and Voltage/Current Harmonic Calculation:

$$THD = \sqrt{\sum \frac{(Harmonic\ Current)^2}{(Fundamental\ Current)^2}} \quad (37)$$

$$I_H = \sqrt{(\sum \frac{(Harmonic\ Current)^2}{(Fundamental\ Current)^2}} \quad (38)$$

Harmonic voltage index can be formulated as:

$$HVI_i = \frac{(Vh_i - V_{ref})}{V_{ref}} \quad (39)$$

The harmonic voltage index (HVI_i) is used to assess the deviation of harmonic voltages (Vh_i) from the reference voltage (V_{ref}) at different nodes. HVI makes it possible to measure the strength of the voltage. It gives a clear idea of how much the voltage waveform is distorted by harmonics. This is very important for figuring out if the voltage is good enough for sensitive equipment and critical loads.

8. CASE STUDIES AND SIMULATION RESULTS

The optimum gain value results from the suggested method are compared to those from many other methods already used in the literature as shown in Table 6 and Figure 6. The table and the Figure both demonstrate that the proposed GWO method is superior.

Table 6 Comparison of gains for PID Controller

Kind of algorithm	Kp	Ki
DE*[26]*	5.0565	9.8298
ABC*[26]*	8.3766	3.7084
HS*[26]*	9.0396	3.6892
PSO*[26]*	7.3216	3.7233
GWO(proposed)	4.8705	9.9654

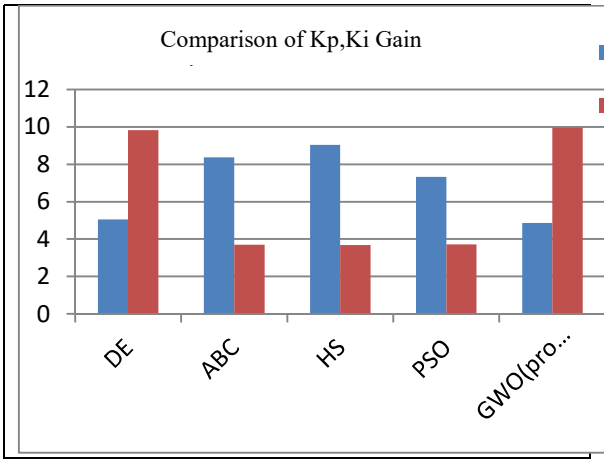

Figure 6: Comparison of Kp,Ki gains with different optimization techniques

Case a: Base case condition

Table 7 PID + GWO Optimal Base Case Conditions for Control Variables

Control Variables	Bus Number	Base case		
		PID	PID+GWO	% decrease in THD
$V_H(\%)$	14	3.8	2.7	28.94
	7	4.5	3.6	20
	10	6.8	5.2	23.52
	9	8.7	4.5	48.27
$I_H(\%)$	14	4.6	3.7	19.56
	7	5.2	4.9	5.76
	10	7.1	6.8	4.2
	9	8.9	7.2	19.10

In the aforementioned reference case, voltage and current harmonic distortion are evaluated at different buses. Bus 14 is where the nonlinear load is wired in. In this situation, the outputs from PID and GWO-based PID controllers are compared. There is a case of uneven load on bus 7.The diode bridge rectifier on bus 10 and the arc furnace on bus 9 are both under consideration.

The proposed controller performance is analyzed in MATLAB/Simulink. Two different loads are considered without & with GWO controller.

Case b: Load performance without GWO controller

Proposed System for Linear Load

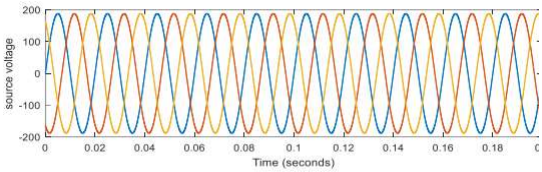

Figure 7: Variation of source voltage

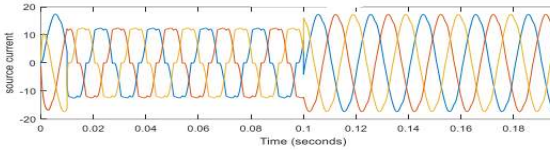

Figure 8: Variation of source current

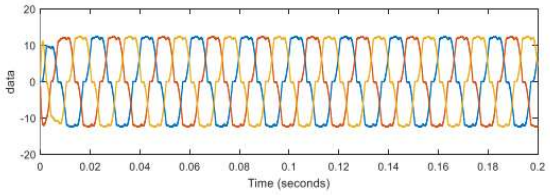

Figure 9: Variation of load current

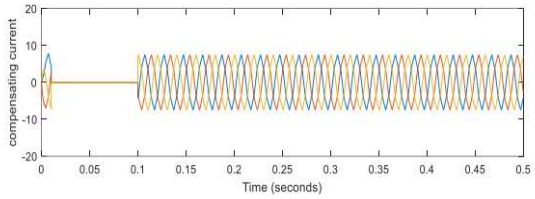

Figure 10: Variation of compensating current

Source voltage, source current, and load current variations are depicted in Figures 7, 8, and 9, with source current distortion visible between (0.01 and 0.1) sec and load-induced distortion becoming less noticeable between 0 and 0.2 sec. The compensator kicks in between periods of time (0.01 and 0.1), during which distortion in the load current is lowest, and continues to do so throughout the rest of the cycle. Figure 10 displays the compensator current.

Proposed System for Unbalanced Load

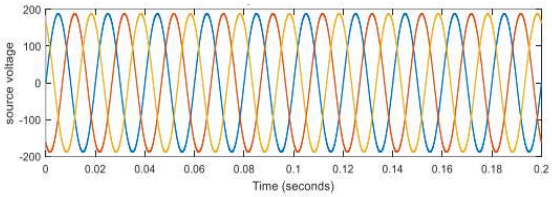

Figure 11: Variation of source voltage

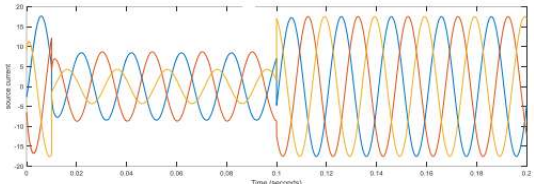

Figure 12: Variation of source current

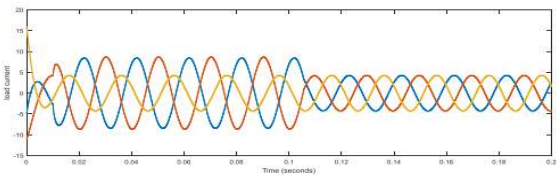

Figure 13: Variation of load current

Variations in source voltage, source current, and load current are depicted in Figures 11, 2, and 13, respectively; Figure 11 shows source current distortion between (0.01 and 0.1) seconds; Figure 2 shows reduced distortion after the load has been started, between 0 and 0.2 seconds. Between zero and tenths of a second, distortion in the load current is lowest, and the compensator is also active throughout the rest of the time the machine is running.

Case c: Load performance with PID+GWO controller

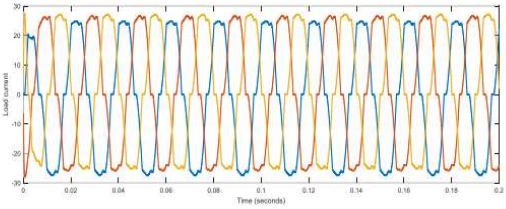

Figure 14: Variation of load current

Load current and compensator current are shown to fluctuate between 0.01s and 0.04s in Figure 14.A compensator is in effect in the system from 0.04s to 0.1s.

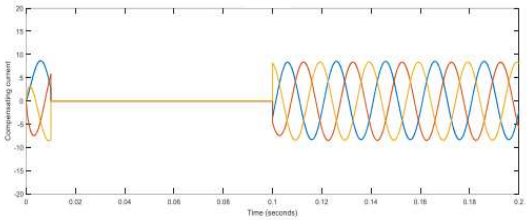

Figure 15: Variation of compensator current

The variation in %VTHD is displayed in Table 8 and Figure 16. When a linear load is taken into account, PID+GWO outperforms PI and PID controllers in terms of fundamental component improvement. For remaining 3 types of considered loads also the chosen controller is shown its importance in terms of %VTHD.

Table8: Variation of %VTHD with various loads

Controller	Linear	Balanced	Diode bridge rectifier	Arc Furnace
PI	1.88	3.64	21.64	75.96
PID	1.75	3.42	19.32	21.64
PID+ GWO	1.53	2.08	17.43	16.55

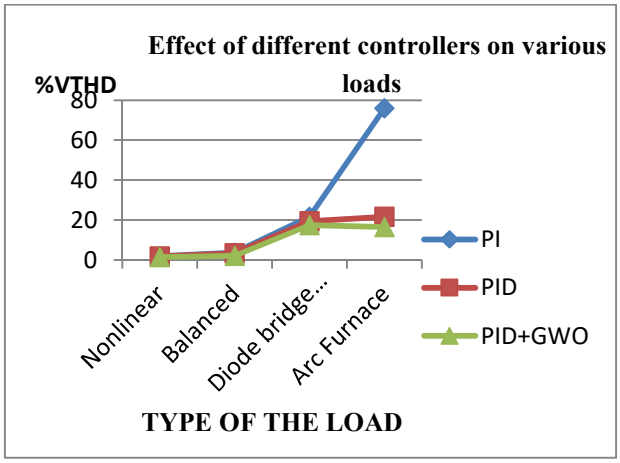

Figure 16: Comparison of Controllers performance for different loads

Table 9: Variation of %ITHD with various loads

Controller	Linear	Balanced	Diode bridge rectifier	Arc Furnace
PI	6.83	4.23	19.89	58.67
PID	6.02	4.04	18.65	19.75
PID+ GWO	5.87	3.84	16.87	14.34

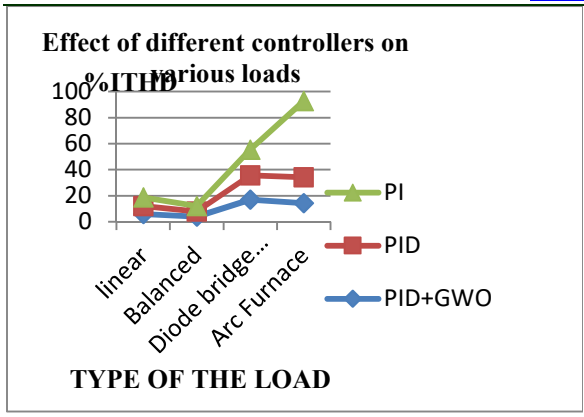

Figure 17: Comparison of Controllers performance for different loads

The variation in %ITHD is displayed in Table 9 and Figure 17. When a linear load is taken into account, PID+GWO outperforms PI and PID controllers in terms of fundamental component improvement. For remaining 3 types of considered loads also the chosen controller is shown its importance in terms of %ITHD.

Table 10: Variation of active power loss with various loads and controllers

Controller	Linear	Balanced	Diode bridge rectifier	Arc Furnace
PID+GWO	3.12KW	1.98KW	9.45KW	8.78KW
PID	3.41KW	2.41KW	11.44KW	22.98KW
PI	3.52 KW	2.63KW	12.64 KW	24.78 KW

Table 10 shows that PID+GWO controllers have lower active power losses than PI and PID controllers.With all the controls in place, balanced loads experience less active power loss than other loads.

Table 11: Comparison of THD for various controllers

Controller	**THD**	**Different Harmonic components as a % of fundamental**	
PID	7.97	Harmonic order	Magnitude(%)
		3rd	**14**
		5th	11
		7th	9.3
		9th	8.2
		11th	7.2
		13th	6.9
		15th	5.2
		17th	**4.2**
PID+PSO	3.97	Harmonic order	Magnitude(%)
		3rd	**10**
		5th	9.1
		7th	8.67
		9th	7.2
		11th	6.4
		13th	5.8
		15th	4.23
		17th	**2.34**
PID+GWO	2.95	Harmonic order	Magnitude(%)
		3rd	**7.54**
		5th	6.23
		7th	5.43
		9th	4.12
		11th	3.09
		13th	2.45
		15th	1.67
		17th	**1.32**

Table 12: Summary of various controllers with different loads

Type of load	Rating of the load	Implemented Controller	%THD(V)	%THD(I)	Active Power loss
Linear load	400 kVA;cos (phi) = 0.8	PI	1.88	6.83	3.52 KW
		PID	1.75	6.02	3.41KW
		PID+GWO	1.53	5.87	3.12KW
Balanced load	320kVA;cos (phi) = 1	PI	3.64	4.23	2.63KW
		PID	3.42	4.04	2.41KW
		PID+GWO	2.08	3.84	1.98KW.
Non Linear load	Diode bridge rectifier	PI	21.64	19.89	12.64 KW
		PID	19.32	18.65	11.44KW
		PID+GWO	17.43	16.87	9.45KW
Non Linear load	Arc furnace	PI	75.96	58.67	24.78 KW
		PID	21.64	19.75	22.98KW
		PID+GWO	16.55	14.34	8.78KW

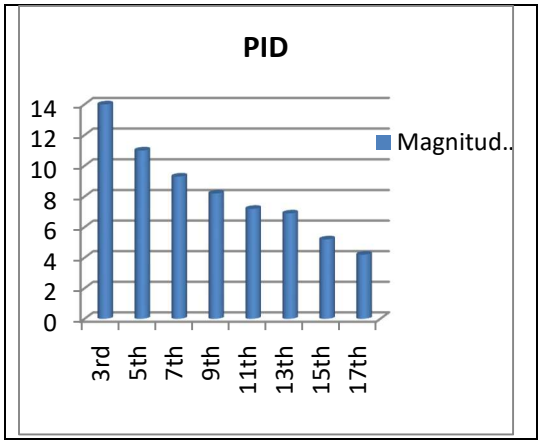

Figure 18: Variation of harmonics with PID

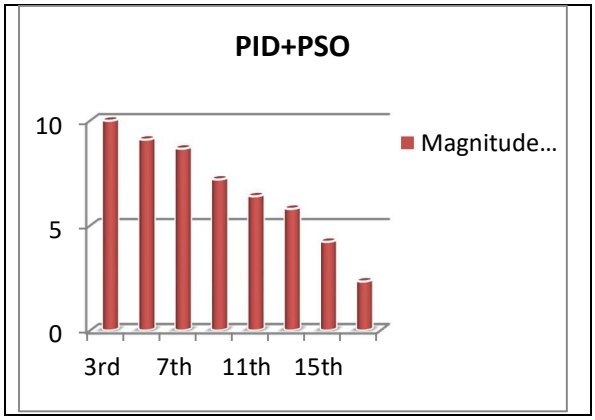

Figure 19: Variation of harmonics with PID+PSO

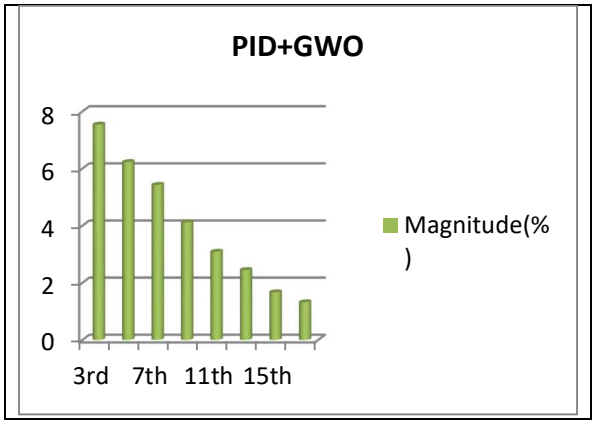

Figure 20: Variation of harmonics with PID+GWO

From Table 11, the best performance of GWO based PID controller reflects in terms of harmonic assessment. Without any optimization, only PID specified 3rd harmonic as 14% of fundamental magnitude and with PSO it is 10% and 7.54% with GWO.

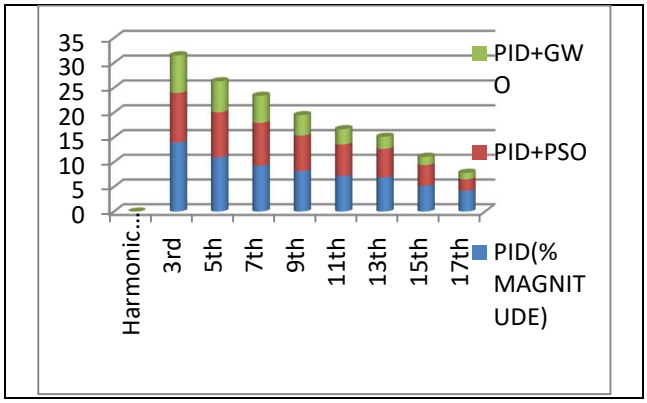

Figure 21: Comparison of harmonics with PID+PSO

The investigated microgrid has bus voltages of ≤69 KV, and the maximum allowable individual harmonic distortion is 3%, as specified by IEEE Standard 519. Harmonic voltage index (HVI) analysis places a premium on harmonics of the 2nd order and lowers the bar as the harmonics progress to the 10th . These indices help assess the quality of voltage with respect to harmonic distortions and provide insights into the potential impact on connected equipment and systems

Table 13:Harmonic voltage index

Harmonic order(n)	Voltage harmonic magnitude (%)	IEEE 519 Limit (%)	HVI
2	8.6	2	3.3
3	7.54	1.5	4.02
4	5.87	0.8	6.33
5	6.23	0.6	9.38
6	5.98	0.3	18.93
7	5.43	0.2	26.15
8	4.99	0.2	23.95
9	4.12	0.1	40.2

ISSN: 1992-8645 www.jatit.org E-ISSN: 1817-3195

We can evaluate the overall effect of harmonic distortions on the voltage quality of the microgrid at a particular bus by looking at this Table 13, which indicates by how much each harmonic component deviates from the required limits.The Harmonic Voltage Index (HVI) is the numerical output of this calculation; it shows the extent to which harmonic voltages surpass safety thresholds for the given harmonic orders. The quality of the power system could be negatively affected by harmonics if the HVI value is significantly higher than the typical range.

This evaluation of harmonic distortion levels provides an overall assessment of the harmonic distortion levels

9. CONCLUSION

The GWO-based PID controller with the SHAPF circuit is presented to address PQ in a grid-connected hybrid system using a battery as the energy storage device. The PID controller's optimal pulses can be achieved with the GWO method. Grey Wolf Optimisation (GWO) was shown to be the best optimization method after being compared to Particle Swarm Optimisation (PSO) in a MATLAB study. GWO's THD value of 2.97 is less than PSO's THD value of 3.05, hence GWO is preferred. That's evidence that GWO can identify a better solution than PSO can. It is also less probable that GWO would become stuck in local optima, and it has a higher convergence rate. In addition to being simpler to build and requiring fewer computer resources, GWO has fewer parameters to tune than PSO. This improves GWO's ability to quickly and accurately address complex optimization problems. The calculated HVI is the main parameter in the harmonic assessment of microgrid.

CONFLICTS OF INTEREST

The authors declare no conflict of interest.

ACKNOWLEDGEMENT

The authors gratefully acknowledge the authorities of Annamalai University for the facilities offered to carry out this work.

AUTHOR CONTRIBUTIONS

Conceptualization, M.Devika Rani; methodology, M.Devika Rani; software, M.Devika Rani; validation, M.Devika Rani, P.S.Prakash, and M.Venu Gopala Rao; formal analysis, M.Devika Rani, P.S.Prakash, and M.Venu Gopala Rao; investigation, M.Devika Rani, P.S.Prakash, and M.Venu Gopala Rao; resources, M.Devika Rani, P.S.Prakash, and M.Venu Gopala Rao; data curation, M.Devika Rani, P.S.Prakash, and M.Venu Gopala Rao; writing—original draft preparation, M.Devika Rani; writing—review and editing, M.Devika Rani, P.S.Prakash, and M.Venu Gopala Rao; visualization, M.Devika Rani, P.S.Prakash, and M.Venu Gopala Rao; supervision, P.S.Prakash, and M.Venu Gopala Rao.

REFERENCES

[1] Xu, J., Zhang, L., Xu, Q., Li, J., & Qian, Z. (2021). Optimal Dispatch Strategy of Hybrid AC/DC Microgrid Considering the Impact of Harmonic Distortion. Energies, 14(17), 5391.

[2] Chen, J., He, Y., Wang, Q., Yuan, Y., & Li, L. (2021). Multi-objective Optimization for Dispatch of Harmonic-Controlled Hybrid AC/DC Microgrid with Energy Storage System. IEEE Transactions on Smart Grid, 12(6), 5569-5581.

[3] Wu, L., Meng, Q., Zhu, L., Chen, X., & Tian, J. (2020). Dispatching Strategy Optimization of AC/DC Hybrid Microgrid Based on Harmonic Analysis. IOP Conference Series: Earth and Environmental Science, 535(3), 032049.

[4] Zhang, Z., Yang, S., Yang, J., Xu, M., & Chen, H. (2020). Optimization Strategy for Active Harmonic Filter in AC/DC Hybrid Microgrid Based on Improved Ant Colony Algorithm. IEEE Access, 8, 115251-115262.

[5] Yu, J., Jiang, J., Chen, C., & Zhou, N. (2019). Optimal Dispatch of AC/DC Hybrid Microgrid Considering Harmonic Distortion and Load Variation. IEEE Access, 7, 160179-160189.

[6] Gholizadeh, M., Sharaf, A.M., & Abdel-Magid, Y.L. (2019). Multi-objective Optimal Dispatch Strategy for Harmonic Mitigation in AC/DC Hybrid Microgrids. International Journal of Electrical Power & Energy Systems, 113, 578-589.

[7] Li, M., Xu, Q., Xu, Y., Zhou, Y., & Qian, Z. (2018). Optimal Dispatch Strategy for AC/DC Hybrid Microgrid Considering Harmonic

Distortion. IEEE Transactions on Smart Grid, 9(4), 3020-3030.

[8] Yao, W., Zhou, J., Jiang, C., Zhou, X. (2020). Enhanced gray wolf optimizer for the optimal dispatch of hybrid microgrid considering uncertainties. Applied Energy, 261, 114303.

[9] Rajan, P.R., Santhi, V., Priyanga, P. (2020). Optimal allocation of hybrid distributed generations in radial distribution system using gray wolf optimizer for power loss reduction. Journal of Electrical Engineering and Technology, 15(1), 384-394.

[10] Zhang, S., Li, Z., Xia, Y., Wang, Z. (2021). Optimal power flow of hybrid AC/DC microgrid with renewable energy sources based on gray wolf optimization algorithm. International Journal of Electrical Power & Energy Systems, 132, 106651.

[11] Yu, B., Gu, W., Yu, M. (2021). Optimal dispatch strategy of hybrid AC/DC microgrid considering distributed energy storage based on improved gray wolf optimizer. Journal of Modern Power Systems and Clean Energy, 9(3), 573-584.

[12] Srinivas, K., Maheshwari, R.P., Saini, J.P., Singh, M. (2021). Optimal scheduling of dispatchable and non-dispatchable DG units in a hybrid AC/DC microgrid using gray wolf optimizer. International Journal of Electrical Power & Energy Systems, 132, 106747.

[13] Bansal, R.C., Bansal, J.C. (2021). Optimal operation of a hybrid AC/DC microgrid using gray wolf optimization algorithm. International Journal of Power and Energy Systems, 41(3), 196-206.

[14] Tan, C., Liu, C., Liao, X., Fang, X., Zhang, X. (2022). Optimal dispatch strategy of hybrid AC/DC microgrid considering multiple objectives based on gray wolf optimizer. Journal of Modern Power Systems and Clean Energy, 10(1), 192-201.

[15] Yang, Y., Xiao, Y., Wang, W., & Yuan, X. (2020). Harmonic assessment and optimization for distributed power generation in a hybrid microgrid. Energies, 13(8), 1995. doi: 10.3390/en13081995

[16] Puri, S., & Singh, R. (2020). Optimization-based harmonic analysis in a distributed power generation system. Journal of Electrical Systems and Information Technology, 7(1), 111-123. doi: 10.2478/jesit-2020-0012

[17] Lu, X., Wang, Z., Huang, Y., & Wu, Q. (2021). Harmonic assessment and optimization of a hybrid microgrid considering uncertainties. IET Generation, Transmission & Distribution, 15(1), 66-74. doi: 10.1049/iet-gtd.2020.0144

[18] Huang, C., Han, X., Yang, X., Zhang, X., & Li, Y. (2020). Harmonic assessment and optimization of a hybrid microgrid based on improved particle swarm optimization. Energies, 13(6), 1449. doi: 10.3390/en13061449

[19] Ramesh, B., & Kumar, P. S. (2021). Optimization-based harmonic analysis and mitigation in hybrid microgrids using multi-objective particle swarm optimization. International Journal of Electrical Power & Energy Systems, 133, 106509. doi: 10.1016/j.ijepes.2021.106509

[20] Singh, G., & Kumar, V. (2020). Harmonic assessment and optimization of a hybrid microgrid using flower pollination algorithm. International Journal of Electrical Power & Energy Systems, 120, 106040. doi: 10.1016/j.ijepes.2020.106040

[21] Jia, H., Li, G., Li, C., & Zhang, G. (2018). Optimal harmonic suppression strategy for a hybrid microgrid based on adaptive genetic algorithm. Energies, 11(11), 3142. doi: 10.3390/en11113142

[22] Yang, J., Li, C., Li, Z., & Pan, Y. (2017). Optimal harmonic control of a hybrid AC/DC microgrid based on particle swarm optimization. Energies, 10(5), 605. doi: 10.3390/en10050605

[23] Abdelaziz, A. Y., Fathy, A. M., & Ahmed, E. H. (2021). Optimal placement of shunt active power filters in microgrid using artificial bee colony algorithm. Electric Power Components and Systems, 49(7-8), 844-854.

[24] Wang, L., Xu, Y., Xia, X., Huang, J., & Zou, J. (2020). Optimal capacitor placement in distribution networks considering distributed generation and load uncertainties using differential evolution. IEEE Transactions on Power Systems, 35(6), 4673-4682.doi: 10.1109/TPWRS.2020.2979606

[25] Sahbasadat Rajamand (2022) Effective Control of Voltage and Frequency in Microgrid Using Adjustment of PID Coefficients by Metaheuristic Algorithms, IETE Journal of Research, 68:5, 3526-3539, DOI: 10.1080/03772063.2020.1769509

[26] Khosravi, N., Abdolmohammadi, H.R., Bagheri, S., Miveh, M.R.: A novel control approach for harmonic compensation using switched power filter compensators in micro-grids. IET Renew. Power Gener. 15, 3989–

4005(2021). https://doi.org/10.1049/rpg2.12317

[27] M. H. K. Roni and M. S. Rana, "Optimized PID Control Scheme for Three Phase Micro-grid System," *2021 2nd International Conference on Robotics, Electrical and Signal Processing Techniques (ICREST)*, DHAKA, Bangladesh, 2021, pp. 77-80, doi: 10.1109/ICREST51555.2021.9331219.

[28] Zishan, F.; Akbari, E.; Montoya, O.D.; Giral-Ramírez, D.A.; Molina-Cabrera, A. Efficient PID Control Design for Frequency Regulation in an Independent Microgrid Based on the Hybrid PSO-GSA Algorithm. *Electronics* **2022**, *11*, 3886. https://doi.org/10.3390/electronics11233886

[29] Murugesan D., Jagatheesan K., Pritesh Shah, Ravi Sekhar, Fractional order PIλDμ controller for microgrid power system using cohort intelligence optimization, Results in Control and Optimization, Volume 11,2023,100218,ISSN 2666-7207, https://doi.org/10.1016/j.rico.2023.100218.

[30] Nisha G and Jamuna K, Frequency Stabilization of Stand-Alone Microgrid with Tuned PID Controller *2022* ECS Transactions, Volume 107, Number 1 DOI 10.1149/10701.0773ecst

[31] Sahbasadat Rajamand (2022) Effective Control of Voltage and Frequency in Microgrid Using Adjustment of PID Coefficients by Metaheuristic Algorithms, IETE Journal of Research, 68:5, 3526-3539. DOI: 10.1080/03772063.2020.1769509